molecular pharmaceutics

Article

pubs.acs.org/molecularpharmaceutics

PEG–Polypeptide Block Copolymers as pH-Responsive Endosome-Solubilizing Drug Nanocarriers

Mohiuddin A. Quadir,[‡] Stephen W. Morton,[‡] Zhou J. Deng, Kevin E. Shopsowitz, Ryan P. Murphy,[†] Thomas H. Epps, III,[†] and Paula T. Hammond*

Department of Chemical Engineering and Koch Institute of Integrative Cancer Research, Massachusetts Institute of Technology, Cambridge, Massachusetts 02139, United States

[†]Department of Chemical and Biomolecular Engineering, University of Delaware, Newark, Delaware 19716, United States

Supporting Information

ABSTRACT: Herein we report the potential of click chemistry-modified polypeptide-based block copolymers for the facile fabrication of pH-sensitive nanoscale drug delivery systems. PEG–polypeptide copolymers with pendant amine chains were synthesized by combining *N*-carboxyanhydride-based ring-opening polymerization with post-functionalization using azide–alkyne cycloaddition. The synthesized block copolymers contain a polypeptide block with amine-functional side groups and were found to self-assemble into stable polymersomes and disassemble in a pH-responsive manner under a range of biologically relevant conditions. The self-assembly of these block copolymers yields nanometer-scale vesicular structures that are able to encapsulate hydrophilic cytotoxic agents like doxorubicin at physiological pH but that fall apart spontaneously at endosomal pH levels after cellular uptake. When drug-encapsulated copolymer assemblies were delivered systemically, significant levels of tumor accumulation were achieved, with efficacy against the triple-negative breast cancer cell line, MDA-MB-468, and suppression of tumor growth in an in vivo mouse model.

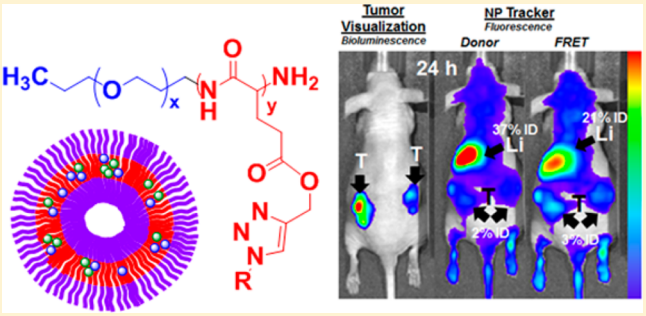

KEYWORDS: *block copolymer, nanocarriers, pH-responsive, drug delivery*

INTRODUCTION

Engineered nanoparticles with stimuli-responsive modalities can substantially improve the therapeutic efficacy of a drug by targeting tumor-specific characteristics, such as hypoxia, for localized delivery of the payload in the desired tissue. A vast arsenal of such nanosystems of either polymeric, liposomal, or micellar origin have been developed and reported following this delivery strategy.[1,2] The working principle of stimuli-responsive drug delivery systems involves a structural or conformational change of the nanocarriers in response to a cellular or extracellular stimulus of chemical, biochemical, or physical origin, resulting in the release of active species within a specific biological environment. Stimuli-responsive nanoparticles provide a critical advantage in delivering payloads to a tissue of interest, where the disease-specific characteristics of that tissue promote drug release, thereby reducing off-target exposure to the therapeutic agent.[3,4]

Among the wide range of biological signals unique to diseased tissue, a change in pH is particularly interesting because of the opportunity to leverage the many pH gradients found in tissues and cellular compartments in both physiological and pathological states.[5,6] Exploitation of the endosomal/lysosomal pH drop has become an established route to improve intracellular delivery and to reduce extracellular toxicity of an active drug that is either conjugated to a polymer backbone through a pH-responsive linker or encapsulated into a pH-responsive nanoparticle.[7] Development of facile, highly controlled fabrication techniques, along with minimal immunogenicity, biodegradability, and clearance of the component polymers, remain a challenge for clinical translation of such pH-responsive systems.[8]

Utilization of a synthetic polypeptide incorporated in a block copolymer with complementary hydrophilic and hydrophobic properties is a promising approach to create self-assembled nanoscale carriers for drug delivery with pH-responsive properties. Stable secondary structures, long-term biodegradability of the peptide bond comprising the polymer backbone, and biocompatibility are some of the attractive features of synthetic polypeptides compared to those of traditional polymers.[9] Synthetic polypeptide-based homopolymers and block copolymers are easily synthesized and provide a facile route to generate hierarchical biocompatible self-assembled superstructures equipped with diverse environmentally sensitive

Received: February 26, 2014
Revised: April 29, 2014
Accepted: May 12, 2014
Published: May 12, 2014

Scheme 1. Synthetic Route to the pH-Responsive Copolymers[a]

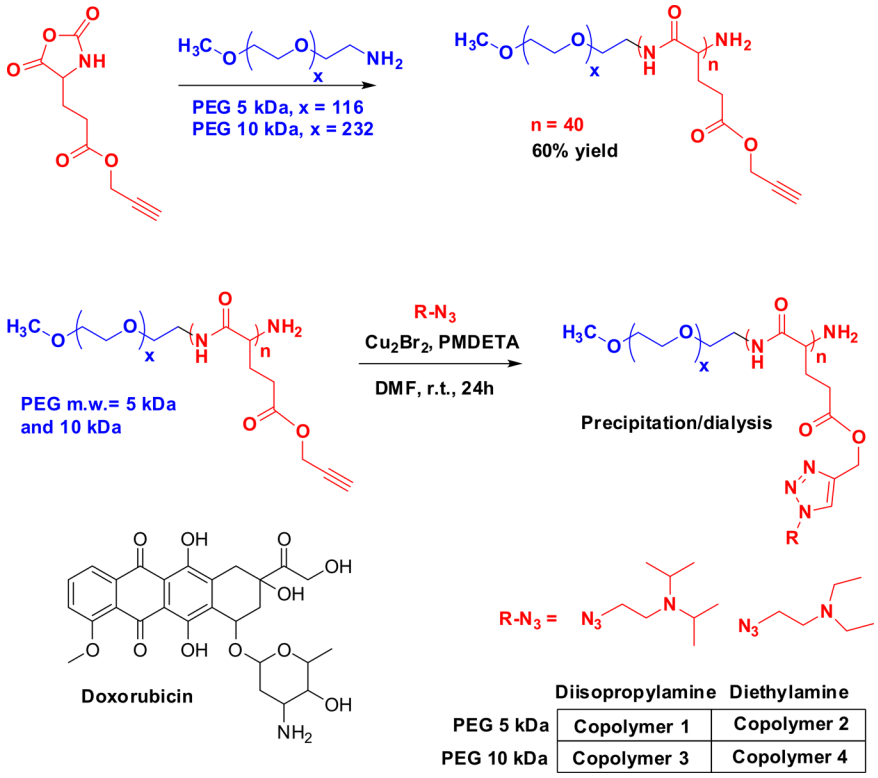

[a]Doxorubicin is used as the model cytotoxic drug.

modalities suitable for biomedical applications.[10−14] Previously, our group reported a new strategy to synthesize poly(γ-propargyl L-glutamate) (PPLG) by *N*-carboxyanhydride (NCA) polymerization of propargyl-L-glutamate.[15] These novel polypeptides contain pendant alkyne groups along the polypeptide chain primed for a facile alkyne−azide cycloaddition (click) reaction; the ability to click virtually any group onto a polypeptide backbone in high density is unique to these systems.[16] In subsequent reports, we described the synthesis of a poly(ethylene glycol)-*b*-PPLG system, in which amine-terminated poly(ethylene glycol) (PEG) was used as an initiator for ring-opening polymerization of the glutamate NCA, thereby creating an amphiphilic block copolymer.[17] By reacting the pendant alkyne side chains on the PPLG backbone with amino-functionalized azides, a library of pH-responsive macromolecules was developed that demonstrates strong buffering capacity with a pH-dependent solubility phase transition in water. These copolymers can aggregate to form stable self-assembled colloids under physiological conditions that remain intact in blood circulation and within the extracellular spaces (pH 7.00−7.45) but that rapidly destabilize under endosomal or highly acidic tumor hypoxic conditions to release a drug payload (early endosome pH 5.5−6.3 and late endosome pH < 5.5). Here, we investigate both the ability of these novel architectures to self-assemble and disassemble in a pH-responsive fashion and examine the effects of this nanocarrier behavior on drug encapsulation and release characteristics in cellular environments. We demonstrate the use of these assemblies as pH-responsive drug delivery systems with optimal pH-controlled stability and release in vitro. Furthermore, we translate these systems to an in vivo murine xenograft model in which we probe the biodistribution, tumor localization, and drug delivery capabilities of these self-assembled carriers toward tumor remediation.

RESULTS AND DISCUSSION

Polypeptide-based self-assembled systems have established themselves as a potential class of drug delivery vehicle, due, in large part, to their stability in systemic circulation and their ability to break down into resorbable amino acids.[18,19] To fabricate polyelectrolyte block copolymers that self-assemble to form pH-responsive nanoparticles, we initiated the ring-opening polymerization of PPLG NCA according to our previous reports,[15,17,20,21] using amine terminal PEG initiators of two different molecular weights, 5 and 10 kDa, to create PEG-*b*-PPLG block copolymers. In subsequent steps, we modified the PPLG block of PEG-*b*-PPLG with two different azido-functionalized tertiary amines, namely, diisopropylamine and diethylamine, by copper catalyzed azide−alkyne cycloaddition, generating copolymers **1**−**4**. The synthetic route to the copolymers is presented in Scheme 1. The efficiency of the click reaction and the attachment of the amine pendant side chains to the polypeptide backbone were confirmed by ^{1}H and ^{13}C NMR spectra that match with our previously reported synthesis.[17] The dispersity of the synthesized copolymers was typically within the range of 1.11−1.16 (Table 1 of the Supporting Information). We chose doxorubicin as a representative chemotherapy drug for assessing encapsulation and release characteristics from these colloidal systems because of the well-defined pharmacological role of the drug in treating several types of cancer and because of its ease of characterization under in vitro and in vivo conditions.

After synthesis of the copolymers, our initial work focused on demonstrating the pH-dependent assembly and disassembly of

dx.doi.org/10.1021/mp500162w | *Mol. Pharmaceutics* 2014, 11, 2420−2430

the PEG-*b*-PPLG copolymers with amine pendant side chains. To that end, critical aggregation concentration (CAC) measurements of the copolymers were performed at four different pH values ranging from 5.5 to 8.0, evaluated by fluorescence spectroscopy using a pyrene probe (Table 1).

Table 1. Critical Aggregation Concentration of Copolymers 1−4 at Different pH Values

	critical aggregation concentration [M]			
pH	copolymer **1**	copolymer **2**	copolymer **3**	copolymer **4**
8.0	7.38×10^{-8}	7.23×10^{-8}	7.44×10^{-7}	8.22×10^{-7}
7.4	7.18×10^{-8}	7.30×10^{-8}	8.07×10^{-7}	8.23×10^{-7}
6.5	n/a[a]	n/a	7.46×10^{-5}	5.82×10^{-5}
5.5	n/a	n/a	n/a	n/a

[a]n/a, not available.

We found that PEG 5 kDa-based copolymers (**1**−**2**) were characterized by CAC values an order of magnitude lower than PEG 10 kDa-*b*-PPLG copolymers (**3**−**4**), indicating more stable assembly of the PEG 5 kDa-*b*-PPLG systems. This finding can be attributed to the increased hydrophilicity and longer length of the PEG 10 kDa chain, which reduces the driving force for assembly. None of the block copolymers exhibited any association at pH 5.5, indicating that the copolymers are able to self-assemble into nanostructures at moderate to high pH but destabilize and disassemble at acidic pH to become unimers as the amines become fully protonated.[17]

Having established the fact that copolymers **1**−**4** show pH-dependent association, we investigated the physical properties of the hierarchical structure that these copolymers form in an aqueous environment. Facile self-assembly of the copolymers was carried out by dissolving 10 wt % of material in DMSO followed by addition of pH 8.0 buffer and subsequent dialysis using a cellulose membrane with a MWCO of 3.5 kDa against a buffer of similar pH for 24 h. The dialyzed solution was passed through a 0.45 μM filter prior to further analysis. Figure 1 illustrates the self-assembly properties of the copolymers after dialysis and filtration. With dynamic light scattering (DLS), it was found that all the copolymers formed nanostructures with characteristic sizes from 110 to 180 nm. The size of the nanoparticles was strongly related to the PEG molecular weight and the pendant amino group side chains (Figure 1a). Recent work has suggested that the morphology of polypeptide-based block copolymer self-assembled structures is not only dependent on the molecular composition but also, to a larger extent, on the kinetic trapping of the system induced by the rigidity of the α-helical hydrophobic peptide segment during the solvent diffusion process.[22] Transmission electron microscopy (TEM) of copolymer **3** (unstained and air-dried on a grid from a solution of nanoparticles at pH 8.0) shows nanoparticles with vesicle-like structures (Figure 1d). (A cryo-TEM image of the vesicles formed from block copolymer **2** is presented in Supporting Information S1a.) We further confirmed the vesicular assembly of the PEG−PPLG pH-responsive vesicles using static light scattering (SLS). The factor $\rho = R_G/R_H$ was calculated for copolymers **1**−**4** from measured values of the radius of gyration (R_G) and radius of hydration (R_H).[22] This value was found to be within the range of 1.02−0.87 (ρ value

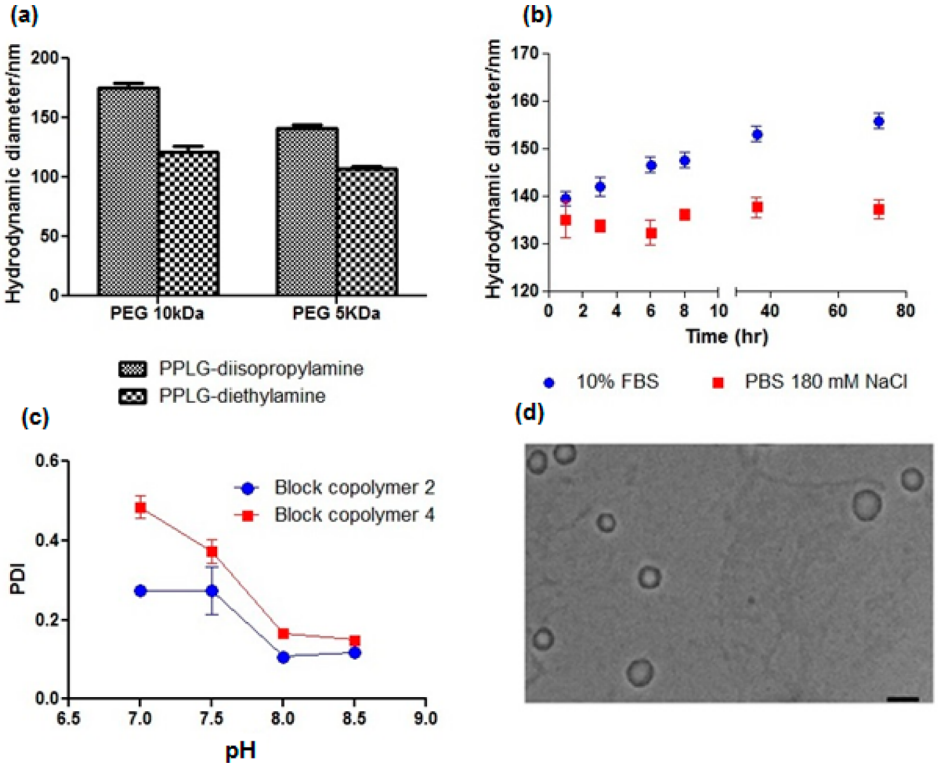

Figure 1. (a) Effect of PEG molecular weight on the hydrodynamic diameter of amine-substituted PEG−polypeptide block copolymer. (b) Effect of serum and salt concentration on the self-assembly of block copolymer **1**. (c) Effect of pH on the polydispersity index of amine-substituted PEG−polypeptide assemblies made of block copolymers **2** and **4**. (d) TEM image of the vesicles synthesized with copolymer **1** at pH 8.0 with a polymer concentration of 1 mg mL^{-1}. The scale bar for the TEM image is 200 nm.

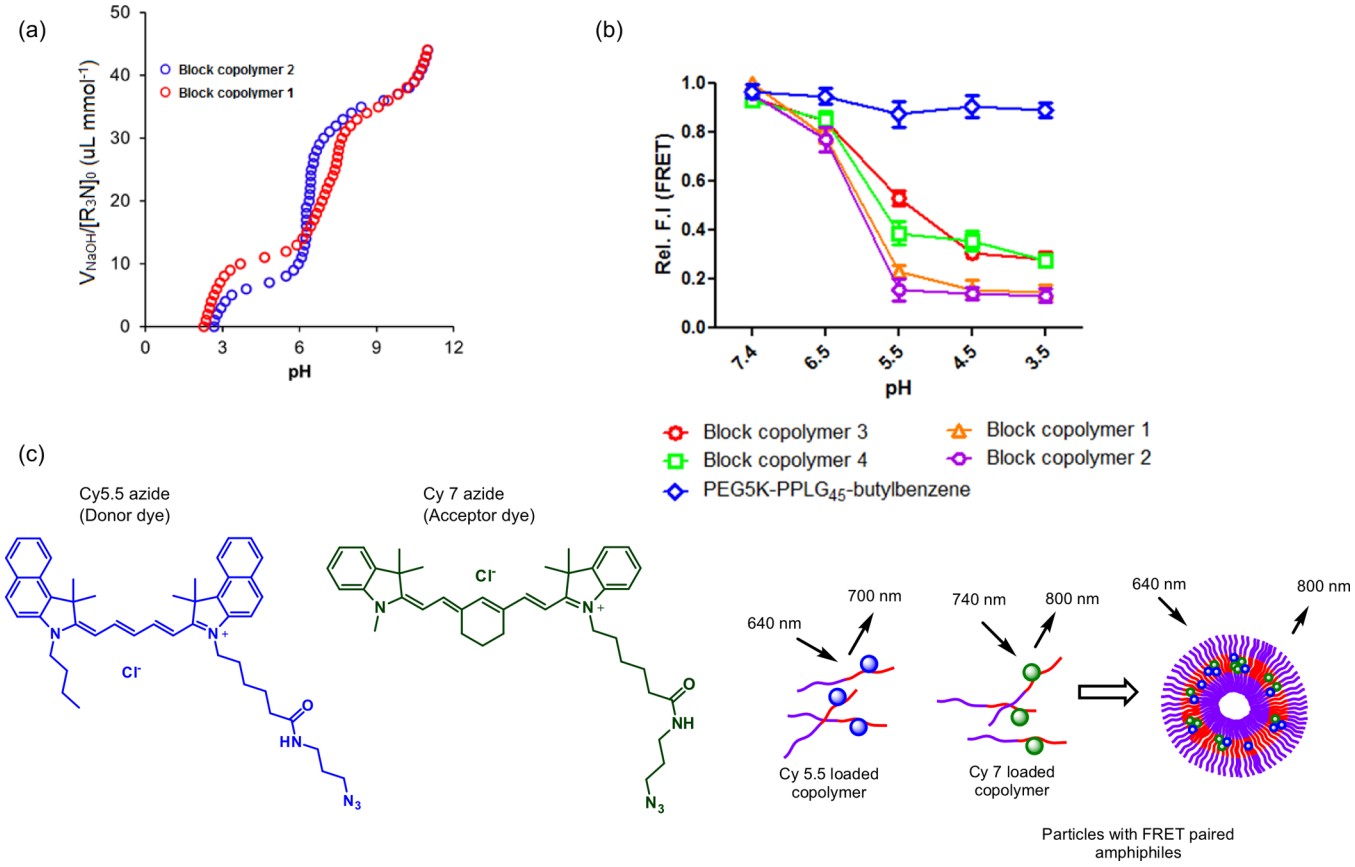

Figure 2. Investigation of pH-responsive properties of representative PEG–polypeptide copolymers. (a) pH titration curve of copolymers **1** and **2**. (b) Reduction of relative FRET efficiency upon lowering the pH from 7.4 to 4.5. (c) Principle of the FRET experiment carried out by forming a vesicle constituted from the respective copolymer tagged with the Cy5.5 and Cy7 FRET pair.

0.733 indicates spherical micellar structures and 1.0 indicates vesicular bilayer constructs). The particles were stable for >1 month in PBS containing 180 mM NaCl, with increased size upon exposure to 10% FBS (Figure 1b for 80 h time period at room temperature). In PBS, the particle size does not change drastically upon elevating the temperature to 37 °C (Supporting Information S1b). The polydispersity indices (PDI) of the vesicles were <0.2 for all **1**–**4** block copolymer systems.

The buffering behavior and pH responsiveness of the PEG–PPLG copolymers with amine pendant chains were investigated with systematic pH titration and Förster resonance energy transfer (FRET)-based experiments. Titration was performed on all four copolymers; the material was dissolved in 125 mM NaCl to partially screen the positive charges on the backbone, and then the pH was gradually increased from 3 to 10. Representative titration curves of copolymers **1** and **2** are presented in Figure 2a. All of the block copolymers under investigation demonstrated a strong buffering capacity from pH 5.5 to 7.7. The pH-induced solubility transition with the addition of acid/base depended strongly on the side chain amine groups, which provide segmental charge repulsion and water solubility.[17] Furthermore, to understand the assembly–disassembly behavior of these systems, a FRET experiment was designed to investigate the pH-responsive property of the vesicles formed from copolymers **1**–**4** (Figure 2c). Utilization of a FRET-associated dye couple is a strategy recently used to investigate the stability of micellar assemblies;[23] in a recent publication, we have shown the ability to use this method to determine the in vivo stability of micelles following intravenous injection in mice.[24] Two fluorophores that are known to form a FRET pair, namely, a Cy5.5 azide and a Cy7 azide, were separately conjugated to approximately 0.1 mol % of unreacted alkyne group present in the PPLG block of an individual copolymer. Then, the Cy5.5 and Cy7 copolymers were blended in solution to form vesicles where FRET coupled dyes are located within the Förster distance. This assembly was achieved by increasing the pH to deprotonate the tertiary amine-containing PPLG block, making it hydrophobic in nature and enabling its self-assembly into nanosized vesicles with the PPLG-amine blocks located in the hydrophobic interior of a vesicular bilayer. The resulting aggregation of the fluorophores brings them within the FRET distance, and excitation of the donor dye at 640 nm causes a fluorescent emission in the FRET channel (800 nm). At lower pH values, the amine groups of the PPLG block become protonated and positively charged, causing vesicular destabilization and substantial reduction in FRET emission because of the increased distance between constituent copolymers that are now free in solution. In comparison, when a pH-nonresponsive copolymer functionalized with butyl benzene was subjected to the same set of experiments, it did not show this pH-dependent reduction of fluorescence emission at lowered pH (Figure 2b).

After establishing the fact that PEG–PPLG copolymers are able to self-assemble into pH-responsive vesicles, we investigated their drug entrapment and release characteristics using doxorubicin, a weak amphipathic water-soluble drug molecule with pK_a = 8.3, as the model drug. Generally, the encapsulation

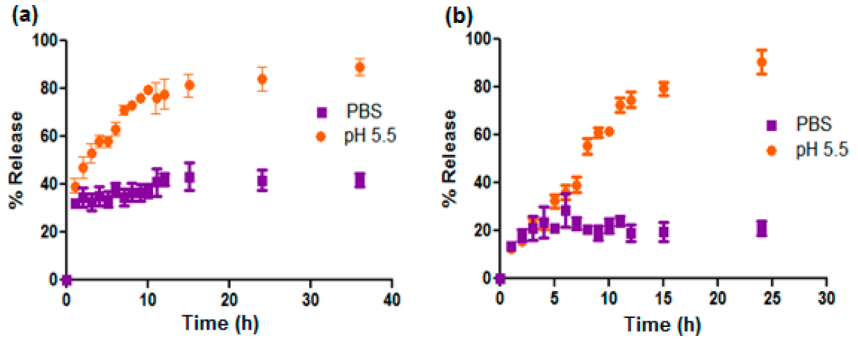

Figure 3. Cumulative release profile of doxorubicin loaded into vesicles formed from (a) copolymer **3** and (b) copolymer **1** in PBS (pH 7.4) and at acidic pH (5.5).

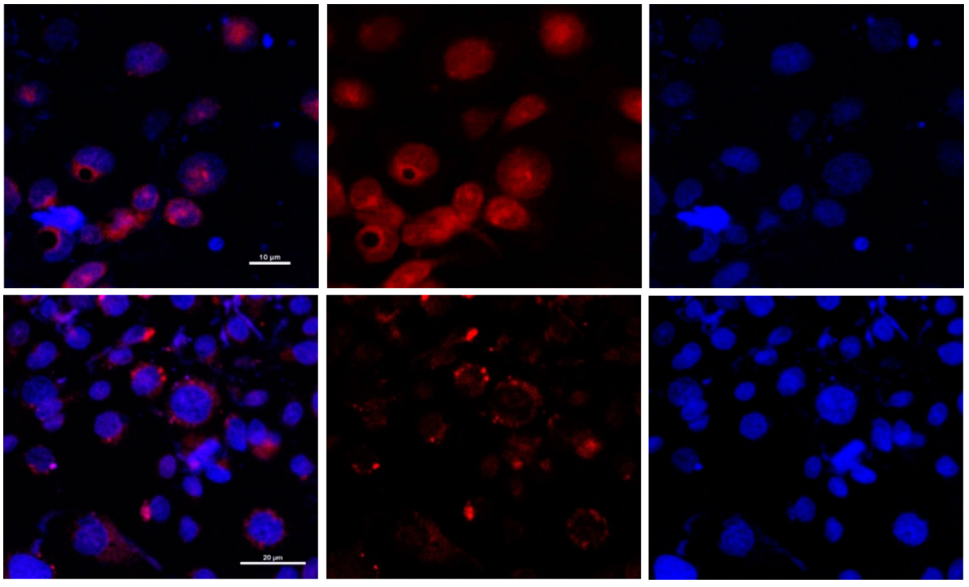

Figure 4. Confocal fluorescence microscopic images of MDA-MB-468 cells treated with doxorubicin-loaded vesicles of copolymer **1** (upper panel) and cells cotreated with the vesicles and 10 μM chloroquine (lower panel) for 2 h at 37 °C. Doxorubicin fluorescence was visualized by excitation at 480 nm and emission at 560 nm.

of doxorubicin within the polymer vesicle core is promoted by applying an ionic or pH gradient across the vesicle membrane.[25−27] We have adapted the protocol from Lecommandoux et al. for encapsulation of doxorubicin within block copolymer vesicles.[28] For the purpose of drug encapsulation, both the copolymer and doxorubicin were dissolved in DMSO followed by gradual and dropwise addition of the DMSO solution to pH 8.0 buffer that was subsequently (time scale of no more than 20 s) introduced to a dialysis medium containing PBS (pH 7.4). The final copolymer concentration was maintained at 2 mg mL^{-1}. After 4 h of dialysis against 10 mM PBS, the doxorubicin loading in vesicles was quantified by UV−vis spectroscopy, and drug release was measured by a dialysis method at two different pH values (PBS of pH 7.4 and 5.5) under sink conditions (37 °C, with constant agitation). In the case of drug encapsulation, it was found that vesicles formed from copolymers **1** and **2** were able to encapsulate 33 and 30% of the added quantity of doxorubicin (i.e., encapsulation efficiency), with a final loading content of 20 and 15% by weight, respectively. Vesicles constituted from copolymers **3** and **4** were able to retain 34 and 31% of the doxorubicin added initially to the copolymer solution during encapsulation; the final loading of these vesicles is 12 and 10% by weight, respectively. In terms of doxorubicin loading, the PEG−PPLG-based vesicles exceed PEO-*b*-polycarbonate block copolymer vesicles[29] and parallel that of other NCA-derived polypeptide block copolymer micellar[30] and vesicular[31] assemblies.

The cumulative release profile of loaded doxorubicin from PEG 10 kDa-based vesicles (constituted from copolymer **3**) showed pH-dependent release between pH 7.4 (PBS) and pH 5.5 (Figure 3a). However, under both of these release conditions, an initial burst release of 40% of total doxorubicin was evident. This burst was followed by a slow release of the drug in PBS, with a more controlled release of drug at pH 5.5. In contrast, the vesicles constituted from PEG 5 kDa-based copolymer **1** released only 20% of entrapped drug after 25 h at pH 7.4 (PBS) and exhibited almost quantitative and sustained release of doxorubicin at pH 5.5 (Figure 3b). In our case, the prominent acceleration of release at pH 5.5 can be attributed to well-reported 3′-NH_2 protonation of the doxorubicin coupled with the protonation of the tertiary amines along the PPLG segment at lower pH, resulting in expulsion of the drug cargo from the vesicle interior.[30] The differences in release behavior between PEG 10 kDa- and 5 kDa-based systems can be attributed to the comparatively reduced stability of the former, as evident from the higher CAC values of copolymer **3** compared to that of **1**. At pH 7.4, doxorubicin release kinetics

dx.doi.org/10.1021/mp500162w | *Mol. Pharmaceutics* 2014, 11, 2420−2430

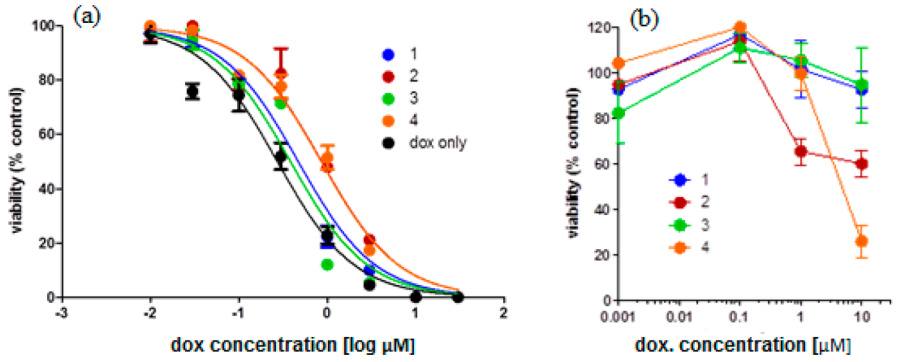

Figure 5. Assessment of efficacy of vesicle-loaded doxorubicin in MDA-MB-468 cells. (a) Concentration-dependent inhibition of four different formulations of vesicles on tumor cell growth. Free doxorubicin was used as a control. (b) Cytotoxicity of the empty vesicles. The concentrations of the vesicles were normalized to their corresponding doxorubicin loading in panel a. The experiments were performed in triplicate, and data are presented as the mean ± standard deviation.

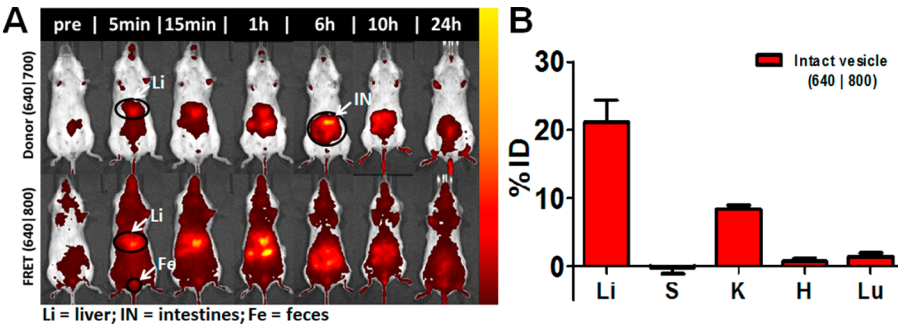

Figure 6. (A) Copolymer **1** vesicle stability on the basis of FRET association of the carrier components following systemic administration in non-tumor-bearing BALB/c mice. Top panel corresponds to λ_{ex} = 640 nm and λ_{em} = 700 nm (donor channel), and bottom panel corresponds to λ_{ex} = 640 nm and λ_{em} = 800 nm (FRET channel). (B) Biodistribution quantitation in necropsied tissue (Li, liver; S, spleen; K, kidneys; H, heart; and Lu, lungs) 24 h following systemic administration in BALB/c mice in both the donor and FRET channels. Fluorescence recovery from harvested tissue includes the background subtraction of tissue from an untreated control for removal of autofluorescence. The resultant quantification is normalized to the injected dose, based on the fluorescence intensity of the injected dose following IVIS imaging of the vial pre-injection.

was mainly controlled by solubilization of the hydrophobically stabilized drug from the membrane assembly of the PPLG block followed by diffusion through the outer PEG layer.

Nanoparticles normally enter cells through endocytosis, and while contained in the endosomal compartment, they undergo an environmental pH decrease from early to late endosomes. To examine the effect of the pH responsiveness on doxorubicin release within the intracellular environment, we treated MDA-MB-468 human breast cancer cells with the vesicles and investigated the intracellular trafficking of doxorubicin by confocal microscopy. After 4 h of incubation with doxorubicin-loaded vesicles, the free drug was found to traverse to the nucleus (Figure 4, upper panel). The data suggested that the pH-responsive vesicles were disrupted by the endosomal pH drop; doxorubicin was released from the vesicles and subsequently diffused into the nucleus where it could bind to DNA. When the cells were cotreated with chloroquine, which is a weak base that buffers the endosomal pH and prevents it from lowering, intracellular doxorubicin was found to accumulate in the cytoplasm in punctate form, contained within the endosomal vesicles, without any translocation to the nucleus (Figure 4, lower panel). This result suggests that the vesicles remain intact inside the endosomes, which is consistent with the pH-responsive properties of the vesicles in the intracellular environment.[31,32]

Next, we assessed the efficacy of the encapsulated doxorubicin in four different vesicular formulations. MDA-MB-468 cells were treated with increasing concentrations of vesicle-loaded doxorubicin for 3 days at 37 °C (Figure 5A), and cell viability was measured at the end of the treatment to generate IC_{50} values for each of the tested formulations. Doxorubicin-loaded vesicles synthesized from copolymers **1**, **2**, **3**, and **4** showed IC_{50} values of 0.85, 0.38, 0.86, and 0.47 μM, respectively. In comparison, free doxorubicin gave a lower IC_{50} value of 0.27 μM. The cytotoxicity of empty vesicles also was assessed, as shown in Figure 5B. The vesicles without doxorubicin were found to be nontoxic to cells within the relevant drug-encapsulated vesicle concentration range. At higher concentrations, vesicles fabricated from copolymers **2** and **4** were found to be more cytotoxic than those prepared from **1** and **3**, which is most likely due to the reduced shielding of the tertiary amino group by aliphatic side chains.

To assess the in vivo stability of the vesicles synthesized from polypeptide-based systems, we used FRET association of Cy5.5 and Cy7 dye-conjugated PEG-*b*-PPLG copolymers using our previously published approach.[24] Copolymer **1** tagged with this FRET dye pair was mixed in stoichiometric proportions at pH 8.0. The solution was dialyzed against PBS at pH 7.4 for 4 h to induce self-assembly. The design of the experiment was motivated from the fact that the dissociation of the vesicles will increase the distance between donor and acceptor dyes, hence reducing the fluorescent intensity in the FRET channel (λ_{ex} = 640 nm; λ_{em} = 800 nm) and increasing the intensity in the donor channel (λ_{ex} = 640 nm; λ_{em} = 700 nm) and thereby

dx.doi.org/10.1021/mp500162w | *Mol. Pharmaceutics* 2014, 11, 2420−2430

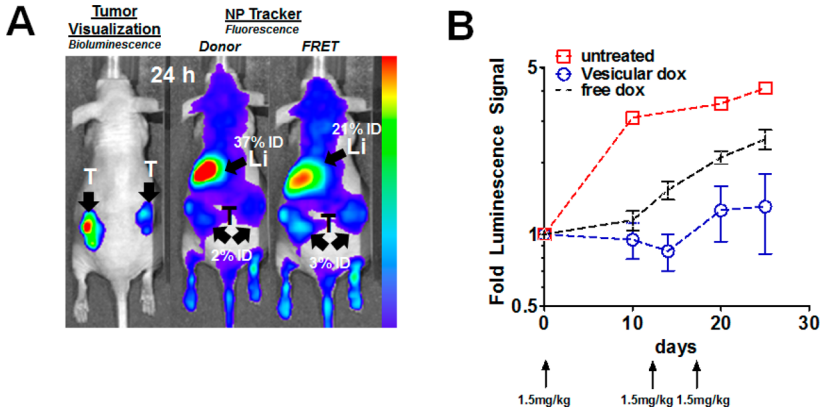

Figure 7. (A) Biodistribution of tumor-bearing nude mice at 24 h post-systemic administration. The left image corresponds to the luminescence of the tumor cell line (MDA-MB-468). The image in the midpanel corresponds to fluorescence imaging of NPs at λ_{ex} = 640 nm and λ_{ex} = 700 nm (donor channel), and the right image corresponds to fluorescence imaging of NPs at λ_{ex} = 640 nm and λ_{ex} = 800 nm (FRET channel). (B) Tumor remediation study against MDA-MB-468 xenografts in NCR nude mice, comparing untreated free-doxorubicin-treated and dox-loaded PEG−PPLG systems treated groups. Data normalized to pre-injection tumor luminescence show a temporally resolved fold change in tumor-specific luminescence signal.

provide a visual and quantifiable readout of the intact vesicle during systemic circulation. The vesicles were systemically administered in BALB/c mice at an injection volume of 0.1 mL at polymer concentrations of 1 mg/mL. The initial pre-injection FRET efficiency of the vesicular formulation in PBS (ex vivo, IVIS, Xenogen) was calculated to be 92%. Biodistribution (Figure 6A,B and Supporting Information Figure S2) and circulation persistence readouts were generated by whole-animal fluorescence imaging, as well as quantification of fluorescence recovery from live-animal blood samples obtained retro-orbitally, in both the donor (λ_{ex} = 640 nm; λ_{em} = 700 nm) and FRET channel (λ_{ex} = 640 nm; λ_{em} = 800 nm). The upper panel of Figure 6A shows the donor channel, indicating that dissociated donor-labeled copolymer cleared fairly rapidly, likely because of its positive charge. The donor fluorescence contributions could additionally be due to swelling or size increase of the vesicles under stress in the systemic biological in vivo environment, although we believe this contribution to be minimal relative to complete dissociation of the micellar structure. The lower panel of Figure 6A illustrates that the associated vesicles are quite stable (higher FRET efficiency, data shown in the Supporting Information) and remain in the bloodstream at appreciable levels for up to 24 h. The persistence characteristics in serum, shown in Figure S3 (Supporting Information), correspond to that of the blood sampled at the time points indicated (Figure 6A). FRET efficiency of isolated serum was obtained from these data. This efficiency was calculated as the ratio of total FRET radiant efficiency to the total radiant efficiency in the donor and FRET channels following background subtraction of whole-animal autofluorescence in the respective channels. These images and the quantified data convey a real-time assessment of these systems as delivery vectors, with pharmacokinetic data on the ability of these systems to remain intact in the bloodstream collected simultaneously with a clearance profile for both destabilized and intact micelles. A rapid destabilization and clearance was noted upon systemic administration (clearing nearly 60% injected dose (ID) from circulation within 30 min and FRET efficiency of 12% for those remaining in the bloodstream); however, a significant fraction was retained in blood (6%) after 24 h with a high FRET efficiency (42%). After 24 h, it was found that 21% ID distributed to the liver and 8% to the kidneys (on the basis of FRET), with minimal fractions detected in other relevant organs (Figure 6B). Similar liver accumulation has been widely reported across the broad architectural spectrum of synthetic nanoparticles. For instance, transferrin-conjugated pegylated gold nanoparticles reported by Choi et al. showed that 17−21% of the initial ID accumulated in the liver, whereas typical NCA-derived polypeptide block copolymer polymersomes, such as a poly(γ-benzyl L-glutamate)-*b*-hyaluronan-based system, showed liver accumulation of 36.54 ± 4.13% ID (per gram of tissue) after 1 h and approximately 33% ID after 24 h, as traced by radioactivity of ^{99m}Tc in Balb/C mice at a 5 mg/kg tail vein injection.[33,34]

After investigating the pharmacokinetics of the carrier based on copolymer **1** in BALB/c mice, we sought to understand the potential of these systems to deliver therapeutics to solid tumors. Using a model with immune-compromised NCR nude mice with established xenografts, we expected the biological performance of the carrier to facilitate delivery to solid tumors for therapy. Investigation of tumor localization of the FRET-assembled system showed significant accumulation in the hind flank tumor xenografts 24 h following systemic administration, displayed in Figure 7A. On the basis of quantification of the FRET-based fluorescence increase post-administration after 24 h, 3% ID localized in the tumor. On the basis of donor fluorescence, 2% ID was observed to be localized in the tumor. In total, 5% ID of the total micelles administered, both destabilized and intact, was found to accumulate, presumably via the enhanced permeation and retention (EPR) effect, in the MDA-MB-468 xenografts. This number is similar to the extent of tumor accumulation exhibited by transferrin-mediated actively targeted gold nanoparticles, where the tumor amassed 2 to 3% of the ID in mice bearing s.c. Neuro2A tumors.[33] It is anticipated that with the use of targeting ligands that enhance uptake, greater accumulation can be achieved with these nanoparticle systems.

Complementary bioluminescence imaging displays the established tumor, with corresponding fluorescence biodistribution data shown to the right, visibly confirming localization of the vesicles in the tumors as well as the anticipated accumulation in liver.

To interrogate the remediation potential of this system, luciferase-expressing MDA-MB-468 xenografts were established

prior to treatment (Figure S4, Supporting Information). The development of these tumors was tracked via live-animal luminescence imaging prior to the systemic administration of 1.5 mg/kg doxorubicin-loaded PEG−PPLG vesicles with three repeated doses at days 0, 10, and 14 following determination of established, progressing solid tumors. As shown in Figure 7B, this treatment regimen reduced tumor growth, whereas the untreated control exhibited exponential growth during this time period. Data are shown as fold luminescence change normalized to pre-injection tumor radiance (based on luminescence imaging of the luciferase-expressing cells). Comparison of days 10 and 20 shows differences in fold luminescence change from the initial tumor size, with the treated group characterized by an average fold change of 0.95 and 1.26 relative to 3.10 and 3.54 for the untreated group (each group is normalized to the tumor-specific luminescence prior to treatment). This observation holds promise considering the fact that tumor growth reduction was achieved at a lower dose (1.5 mg/kg, three doses) than previously reported polypeptide-based doxorubicin polymersomes, for which 5 mg/kg (single dose) was required to delay the doubling time of tumor growth.[34]

■ CONCLUSIONS

We have shown that novel PEG−polypeptide copolymers with amine pendant chains can be utilized as a pH-responsive drug delivery vehicle. These copolymers can self-assemble as vesicles that are effective systemically administrable drug carriers. Furthermore, the vesicles are able to encapsulate therapeutically significant quantities of drug and to release them in a pH-dependent manner in the intracellular environment. We also have demonstrated that these nanosized vesicles are stable platforms for delivery and can successfully localize in solid tumors and release doxorubicin, mediated by the enhanced permeation and retention effect and the lowered pH of the tumor microenvironment. When loaded with doxorubicin, the vesicles were found to reduce tumor growth, whereas the untreated control tumors continued to grow exponentially. Currently, we are investigating the effect of different hydrophobic and hydrophilic segments of the constituent block copolymers on in vivo residence time, and we are exploring the targeting and drug delivery efficacy of the vesicles in tumor-bearing animal models. It is anticipated that these systems can be labeled with molecular targeting ligands that further enhance tumor specificity while lowering uptake in other parts of the body.

■ METHODS AND MATERIALS

Synthesis of PEG−Polypeptide Block Copolymer with Alkyl Amine Side Chains. The synthesis of PEG−-polypeptide block copolymer was carried out by previously described methods.[17] As a representative example of PEG5K−PPLG copolymer (**1**), first, γ-propargyl L-glutmate was prepared by esterification of L-glutamic acid with propargyl alcohol using TMSCl (trimethylsilyl chloride) as the coupling agent. L-Glutamic acid (20.6 g, 140 mmol, 1.0 equiv) was first suspended in propargyl alcohol (31.0 g, 140 mmol, 1.0 equiv), and the reaction mixture was cooled to 0 °C. Then, TMSCl (38 g, 350 mmol, 2.5 equiv) was added dropwise, and the reaction was allowed to run for 48 h under a nitrogen environment. The resultant product, propargyl L-glutamate, was purified by precipitation of the reaction mixture in diethyl ether followed by filtration. In the second step, propargyl-L-glutamate was converted to its corresponding *N*-carboxyanhydride by the well-established Fuchs−Farthing method, whereby propargyl L-glutamate (5.1 g 23 mmol, 1.0 equiv) was decarboxylated by triphosgene (2.61 g, 8.7 mmol, 0.38 equiv). The ring-opening polymerization of the resulting propargyl L-glutamate NCA (3.8 g, 18.3 mmol, 25 equiv) was initiated with amine-terminated poly(ethylene glycol) of different molecular weights (MW 5K and 10K) under a nitrogen atmosphere. The polymerization reaction was allowed to continue for 72 h, after which the resulting poly(ethylene glycol)-*b*-poly(γ-propargyl L-glutamate) (PEG-*b*-PPLG) was purified by repeated precipitation in diethyl ether and water. Two types of azide-modified amine side chains, diisopropylamine and diethylamine, were conjugated to the polymer backbone by a Cu-mediated azide−alkyne click cycloaddition reaction. As a typical example of a click cycloaddition reaction, a PEG-*b*-PPLG block copolymer (1.7 g, 2.3 mmol, 1.0 equiv of alkyne repeat units) was dissolved in anhydrous DMF, into which azide-terminated amines (2.0 g, 3.5 mmol, 1.5 equiv of alkyne repeat units) and PMDETA (0.2 g, 1.2 mmol, 0.5 equiv) were successively added. The resulting solution was degassed by bubbling nitrogen through the solution for 10 min, after which CuBr (0.172 g, 1.2 mmol, 0.5 equiv) was added. The reaction was allowed to run at room temperature under nitrogen atmosphere for 48 h, after which the solvent was evaporated, and the residue was dissolved in acidified water and treated with dowex M1341 for 15 min. After removal of the dowex beads by filtration, the solution was dialyzed against acidified water (pH < 5.0) for 24 h followed by dialysis against Milli-Q water. After freeze-drying, the final polymer was obtained as an off-white solid with an overall yield of 65%. Spectral data match with those of previously reported compounds.[15,17]

Fabrication and Characterization of Block Copolymer Vesicles. The block copolymer vesicles were fabricated by a diafiltration method as previously reported.[22,28] Briefly, 30 mg of amine-substituted PEG-*b*-PPLG was first dissolved in 1 mL of DMSO with stirring for 30 min. Then, the solution was added dropwise to 2 mL of phosphate buffer at pH 8.0 with stirring. The resulting mixture was stirred at room temperature for another 1 h, after which it was dialyzed against pH 8.0 buffer for 48 h to promote self-assembly. The dialysis medium was changed every 4 h for the first 12 h. The concentration of the polymers after dialysis was 6 mg/mL. The dialyzed self-assembled vesicles suspension was filtered through 0.45 μm polyether sulfone filters and analyzed using dynamic light scattering (DLS; Malvern Instruments Ltd., UK) to determine particle size. For multiangle light scattering measurements, a Brookhaven instrument was used at scattering angles of 30 to 150° with a 1 min measurement time/sample. The cumulant analysis method (DLS) was used to determine the hydrodynamic diameter and polydispersity of the vesicles, and static light scattering (SLS) was used to determine the radius of gyration (R_G). TEM images were captured with a JEOL 2010 advanced high-performance TEM at an acceleration voltage of 200 keV. Samples were prepared by drop-casting 2 μL of a 10 mg/mL vesicle suspension onto a carbon-coated 200 mesh copper grid. Cryo-TEM images were captured using a Tecnai G2 12 Twin TEM operating at 120 kV, with a sample probe temperature below −176 °C during imaging. Samples were prepared using an FEI Vitrobot at 22 °C and 100% relative humidity. A 3 μL sample volume was pipetted onto plasma-

etched Quantifoil R 2/1 grids prior to blotting and subsequent vitrification in liquid ethane.

Acid−Base Titration and Assessment of pH-Dependent Aggregation Behavior. Acid−base titration was performed by gradual change of pH from 3 to 10 through the incremental addition of 0.1 M NaOH according to published procedures.[32,35] Amine-substituted PEG-*b*-PPLG copolymers were dissolved in 3 mL of 125 mM NaCl solution, with an amine concentration equivalent of 10 mM. The pH of this solution was reduced to 3.0 using 1 M HCl. The titration was carried out by adding 10 mL aliquots of 0.1 M NaOH to the resulting acidic solution of PEG-*b*-PPLG and measuring the pH after every addition. To determine the pH-dependent aggregation behavior, critical association concentration (CAC) values of the diblock copolymers were measured spectrofluorometrically as a function of pH using the pyrene probe method. A stock solution of pyrene in acetone (6.5×10^{-5} M) was prepared, and 10 μL aliquots were added to glass vials. After allowing the acetone to evaporate, polymer solutions at different concentrations prepared in pH 5.5, 6.5, 7.4, and 8.0 buffers were added to the vials and left to equilibrate overnight. The final concentration of pyrene in the working solution was kept at 6.5×10^{-7} M. The ratio of the peak intensities of fluorescence emission (373/384 nm) was used to determine the CAC as a function of pH. Fluorescence spectroscopy was carried out on a Horiba Fluorolog spectrofluorimeter at room temperature. For FRET-based assessment of pH-dependent aggregation−disaggregation, Cy5.5- and Cy7.0-conjugated pH-responsive block copolymers were first synthesized by attaching azide-terminated dyes to unreacted alkyne side chains (0.1 mol %) by copper-mediated click chemistry. Dye-labeled vesicles were first dissolved in phosphate buffer of pH 8.0 with a final block copolymer concentration of 5 mg/mL. The stock solution was diluted with 0.2 M citric−phosphate buffer to different pH values, keeping the final polymer concentration fixed at 1 mg/mL. A pH-nonresponsive block copolymer ($PEG\text{-}NH_2$ initiated PPLG block copolymer with aromatic side chains) was used as control. The solutions were excited at 640 nm, and emission spectra were collected from 780 to 810 nm with excitation slits at 5 nm. The emission intensity at 800 nm was used to determine the pH-responsive aggregation behavior of the block copolymer assembly.

Doxorubicin Loading and Release Experiment. The loading of doxorubicin into the vesicles was performed as previously described,[28] and their pH-dependent release behavior was assessed following a previously reported protocol.[28] Briefly, 10 mg of block copolymer was codissolved with a specific amount of doxorubicin in 0.5 mL of DMSO. The organic phase was gradually and dropwise added to phosphate buffer of pH 8.0 with stirring followed by rapid transfer to a dialysis bag immersed in PBS (pH 7.41, ionic strength 150 mM). To remove the excess drug and DMSO, dialysis was carried out using a membrane with a MWCO of 3.5 kDa for 4 h at 30 °C. Drug loading content was quantified by measuring the absorbance at λ_{max} = 488 nm in PBS with the use of a calibration curve. The loading efficiency is generally expressed as the percent mass of doxorubicin in vesicles relative to the mass of doxorubicin in the initial solution, and loading content is expressed as the percent mass of doxorubicin in vesicles relative to the mass of the block copolymer. For the release experiments, spectra/Por 10 kDa MWCO float-a-lyzers (1 mL volume) were loaded with 1 mL of a doxorubicin-containing vesicle suspension. The float-a-lyzer arrangement was either introduced to 25 mL of PBS (pH 7.4) or, for release experiments at pH 5.5, the content within the dialysis container was acidified to pH 5.5 and then immersed in 25 mL of dialysis medium composed of pH 5.5 acetate buffer (10 mM acetate, ionic strength 150 mM). With the maintenance of sink conditions by replacing 2 mL of the dialysis medium with fresh medium, the residual drug was measured by taking an aliquot from inside the dialysis bag and measuring absorbance at λ_{max} of 488 nm. The percentage of drug release was calculated from the following equation:[28]

$$\%\ \text{drug release} = \left(1 - \frac{\text{absorbance}(t)}{\text{absorbance}(t_0)}\right) \times 100$$

In Vitro Experimentation. *Cytotoxicity Studies.* MDA-MB-468 triple-negative breast adenocarcinoma cells (ATCC) were used in our experiments and grown in DMEM media supplemented with 10% fetal bovine serum, 50 units/mL penicillin, and 50 units/mL streptomycin.

Cytotoxicity assays were performed using the CCK-8 cytotoxicity assay (Sigma). Briefly, cells were seeded in a 96-well plate at 30% confluence, and after 24 h, they were treated with the vesicles at various concentrations. After 3 days of incubation, the cell medium was replaced with fresh serum-free OptiMEM medium containing 10% v/v of the CCK-8 proliferation reagent. After 2 h of incubation at 37 °C, the absorbance at 450 nm was measured by a plate reader. Cell viability was normalized to an untreated control and calculated using a standard curve. To study the efficacy of doxorubicin-containing vesicles, the data were fit with a dose-dependent inhibition curve using Prism 5 (GraphPad).

Confocal Microscopy. Cellular uptake of PEG−PPLG vesicles was assessed by confocal fluorescence microscopy. The confocal microscope images were taken using a Nikon A1R ultra-fast spectral scanning confocal microscope (Nikon Instruments Inc., Melville, NY). Cells were seeded in CELLview glass-bottom dishes (Greiner Bio-One GmbH, Germany) at 1×10^5 cells per well and grown overnight. Then, cells were incubated with the vesicles at 37 °C in DMEM complete medium for 24 h. At the end of this period, cells were washed followed by addition of DAPI for an additional 10 min, after which they were further washed with PBS and imaged.

In Vivo Experimentation. *FRET Stability Studies.* FRET assembled PEG−PPLG vesicles were systemically administered in BALB/c mice (0.1 mL via tail vein injection) at a concentration of 1 mg/mL (FRET radiant efficiency = 1×10^9). Temporally resolved biodistribution imaging was performed using an IVIS live-animal fluorescence imaging system at both the specified donor and FRET channels (Xenogen, Caliper Instruments). Quantification of radiant efficiency was performed by drawing regions of interest around the collected blood samples using Living Image 4.0 software (Caliper). Data presented as the percent ID were determined by quantifying total radiant efficiency of the injected sample (determined by imaging prior to administration) and calculating the fraction remaining by the total fluorescence recovery from serial bleeding (with background subtraction of an untreated control blood sample for autofluorescence determination). Necropsy of the treated mice was performed at 24 h. Organ distribution was determined by quantifying organ-specific recovery of fluorescence above an untreated, autofluorescence control and normalizing that to the injected dose.

Tumor Remediation. Xenografts were established by injecting 0.1 mL of 5×10^7 MDA-MB-468 luciferase-expressing cells in a 1:1 cell suspension with BD Matrigel basement membrane matrix. Tracking of solid tumor growth was monitored by luminescence imaging (Xenogen, Caliper), where at each time point of interest 0.1 mL of 30 mg/kg D-luciferin (Caliper) was administered via i.p. injection to the tumor-bearing mice 15 min prior to imaging (which used an open luminescence filter). Quantification of tumor size was done using Living Image Software, where the total radiance of each tumor was determined by region of interest analysis around the entire xenograft. Data are presented as the mean ± SEM (measured in total radiance) of the fold luminescence change above the baseline pre-treatment tumor size (on the basis of radiance). Each animal was normalized independently and then averaged across the entire group ($n = 4$) for both the treatment and control groups. Tumor-bearing mice receiving the dox-loaded PEG-*b*-PPLG system were given three repeated systemically administered 0.1 mL doses at 1.5 mg/kg on day "0" (after 12 days of tumor establishment and growth phase), 10, and 14.

■ ASSOCIATED CONTENT

Supporting Information

Physicochemical properties of the copolymers, organ biodistribution and blood circulation profiles, and tumor growth curve. This material is available free of charge via the Internet at http://pubs.acs.org.

■ AUTHOR INFORMATION

Corresponding Author

*Email: hammond@mit.edu.

Author Contributions

‡M.A.Q and S.W.M contributed equally to this work, and the manuscript was written through contributions of all authors. M.A.Q. performed the synthesis and physicochemical analysis. S.W.M. carried out the in vivo experimentation and quantification of data. Z.J.D. designed the in vitro experiments. K.E.S. and R.P.M. performed TEM and cryo-TEM. T.H.E. assisted with the design, analysis, and interpretation of DLS and SLS data. P.T.H. designed the experiments and supervised the project.

Notes

The authors declare no competing financial interest.

■ ACKNOWLEDGMENTS

The authors thank Novartis Institutes for BioMedical Research, Inc. for the primary funding of this work. The authors would like to thank the following funding agencies for providing valuable resources to facilitate this work. These include grants from the NIH and Center for Cancer Nanotechnology Excellence (CCNE), grant nos. P30 CA14051 and 5 U54 CA151884-02. The authors would also like to acknowledge the Koch Institute for Integrative Cancer Research at MIT for providing resources (facilities, funding) central to the completion of this work, specifically the Koch Institute Swanson Biotechnology Center core facilities (microscopy, flow cytometry, and whole animal imaging) for facilitating the acquisition of biological data, the MIT Department of Comparative Medicine (DCM) for husbandry and general animal care, and the Institute of Soldier Nanotechnology (ISN) at MIT for instrumental support. S.W.M. would like to acknowledge support from an NSF graduate research fellowship. K.E.S. would like to thank the NSERC for a postdoctoral fellowship. T.H.E. and R.P.M. thank Institutional Development Award (IDeA) from the National Institute of General Medical Sciences of the National Institutes of Health (NIH), grant P20GM103541, for financial support. The statements herein do not reflect the views of the NIH. The authors also acknowledge the W. M. Keck Microscopy Facility at the University of Delaware for use of the TEM and Vitrobot.

■ DEDICATION

The authors wish to dedicate this paper to the memory of Officer Sean Collier, for his caring service to the MIT community and for his sacrifice.

■ ABBREVIATIONS

PEG, poly(ethylene glycol); PPLG, poly(γ-L-propargyl glutamate); NCA, *N*-carboxyanhydride; FRET, Förster Resonance Energy Transfer; CAC, Critical Aggregation Concentration; SEM, Scanning Electron Microscopy; TEM, Tunneling Electron Microscopy; DMSO, Dimethyl sulfoxide; MWCO, Molecular Weight Cut-off

■ REFERENCES

(1) Schroeder, A.; Heller, D. A.; Winslow, M. M.; Dahlman, J. E.; Pratt, G. W.; Langer, R.; Jacks, T.; Anderson, D. G. Treating metastatic cancer with nanotechnology. *Nat. Rev. Cancer* **2012**, *12*, 39−50.

(2) Wang, A. Z.; Langer, R.; Farokhzad, O. C. Nanoparticle delivery of cancer drugs. *Ann. Rev.* **2012**, *63*, 185−198.

(3) Aluri, S.; Janib, S. M.; Mackay, J. A. Environmentally responsive peptides as anticancer drug carriers. *Adv. Drug Delivery Rev.* **2009**, *61*, 940−952.

(4) Ganta, S.; Devalapally, H.; Shahiwala, A.; Amiji, M. A review of stimuli-responsive nanocarriers for drug and gene delivery. *J. Controlled Release* **2008**, *126*, 187−204.

(5) Petros, R. A.; DeSimone, J. M. Strategies in the design of nanoparticles for therapeutic applications. *Nat. Rev. Drug Discovery* **2010**, *9*, 615−627.

(6) Sonawane, N. D.; Szoka, F. C., Jr.; Verkman, A. S. Chloride accumulation and swelling in endosomes enhances DNA transfer by polyamine−DNA polyplexes. *J. Biol. Chem.* **2003**, *278*, 44826−44831.

(7) Mellman, I. The importance of being acid: the role of acidification in intracellular membrane traffic. *J. Exp. Biol.* **1992**, *172*, 39−45.

(8) Whitehead, K. A.; Langer, R.; Anderson, D. G. Knocking down barriers: advances in siRNA delivery. *Nat. Rev. Drug Discovery* **2009**, *8*, 129−138.

(9) Deming, T. J. Synthetic polypeptides for biomedical applications. *Prog. Polym. Sci.* **2007**, *32*, 858−875.

(10) Bonduelle, C.; Huang, J.; Ibarboure, E.; Heise, A.; Lecommandoux, S. Synthesis and self-assembly of "tree-like" amphiphilic glycopolypeptides. *Chem. Commun.* **2012**, *48*, 8353−8355.

(11) Bromley, E. H. C.; Channon, K.; Moutevelis, E.; Woolfson, D. N. Peptide and protein building blocks for synthetic biology: from programming biomolecules to self-organized biomolecular systems. *ACS Chem. Biol.* **2008**, *3*, 38−50.

(12) Chen, C. Y.; Wang, Z. H.; Li, Z. B. Thermoresponsive polypeptides from pegylated poly-L-glutamates. *Biomacromolecules* **2011**, *12*, 2859−2863.

(13) Deming, T. J. Polypeptide and polypeptide hybrid copolymer synthesis via NCA polymerization. *Peptide Hybrid Polymers* **2006**, *202*, 1−18.

(14) Huang, J.; Habraken, G.; Audouin, F.; Heise, A. Hydrolytically stable bioactive synthetic glycopeptide homo- and copolymers by combination of NCA polymerization and click reaction. *Macromolecules* **2010**, *43*, 6050−6057.

(15) Engler, A. C.; Lee, H. I.; Hammond, P. T. Highly efficient "grafting onto" a polypeptide backbone using click chemistry. *Angew. Chem., Int. Ed.* **2009**, *48*, 9334−9338.
(16) Quadir, M.; Martin, M.; Hammond, P. T. Clickable synthetic polypeptides routes to new highly adaptive biomaterials. *Chem. Mater.* **2014**, *26*, 461−476.
(17) Engler, A. C.; Bonner, D. K.; Buss, H. G.; Cheung, E. Y.; Hammond, P. T. The synthetic tuning of clickable pH responsive cationic polypeptides and block copolypeptides. *Soft Matter* **2011**, *7*, 5627−5637.
(18) Peer, D.; Karp, J. M.; Hong, S.; Farokhzad, O. C.; Margalit, R.; Langer, R. Nanocarriers as an emerging platform for cancer therapy. *Nat. Nanotechnol.* **2007**, *2*, 751−760.
(19) Bellomo, E. G.; Wyrsta, M. D.; Pakstis, L.; Pochan, D. J.; Deming, T. J. Stimuli-responsive polypeptide vesicles by conformation-specific assembly. *Nat. Mater.* **2004**, *3*, 244−248.
(20) Chopko, C. M.; Lowden, E. L.; Engler, A. C.; Griffith, L. G.; Hammond, P. T. Highly-tunable multiplexed thermo- and pH responsive polypeptide, submitted for publication.
(21) Chopko, C. M.; Lowden, E. L.; Engler, A. C.; Griffith, L. G.; Hammond, P. T. Dual responsiveness of a tunable thermosensitive polypeptide. *ACS Macro Lett.* **2012**, *1*, 727−731.
(22) Huang, J.; Bonduelle, C.; Thevenot, J.; Lecommandoux, S.; Heise, A. Biologically active polymersomes from amphiphilic glycopeptides. *J. Am. Chem. Soc.* **2012**, *134*, 119−122.
(23) Lu, J.; Owen, S. C.; Shoichet, M. S. Stability of self-assembled polymeric micelles in serum. *Macromolecules* **2011**, *44*, 6002−6008.
(24) Morton, S. W.; Zhao, X.; Quadir, M. A.; Hammond, P. T. FRET-enabled biological characterization of polymeric micelles. *Biomaterials* **2014**, *35*, 3489−3496.
(25) Harrigan, P. R.; Wong, K. F.; Redelmeier, T. E.; Wheeler, J. J.; Cullis, P. R. Accumulation of doxorubicin and other lipophilic amines into large unilamellar vesicles in response to transmembrane pH gradients. *Biochim. Biophys. Acta* **1993**, *1149*, 329−338.
(26) Madden, T. D.; Harrigan, P. R.; Tai, L. C.; Bally, M. B.; Mayer, L. D.; Redelmeier, T. E.; Loughrey, H. C.; Tilcock, C. P.; Reinish, L. W.; Cullis, P. R. The accumulation of drugs within large unilamellar vesicles exhibiting a proton gradient: a survey. *Chem. Phys. Lipids* **1990**, *53*, 37−46.
(27) Bally, M. B.; Mayer, L. D.; Loughrey, H.; Redelmeier, T.; Madden, T. D.; Wong, K.; Harrigan, P. R.; Hope, M. J.; Cullis, P. R. Dopamine accumulation in large unilamellar vesicle systems induced by transmembrane ion gradients. *Chem. Phys. Lipids* **1988**, *47*, 97−107.
(28) Sanson, C.; Schatz, C.; Le Meins, J. F.; Soum, A.; Thevenot, J.; Garanger, E.; Lecommandoux, S. A simple method to achieve high doxorubicin loading in biodegradable polymersomes. *J. Controlled Release* **2010**, *147*, 428−435.
(29) Chen, W.; Meng, F.; Cheng, R.; Zhong, Z. pH-sensitive degradable polymersomes for triggered release of anticancer drugs: a comparative study with micelles. *J. Controlled Release* **2010**, *142*, 40−46.
(30) Kataoka, K.; Matsumoto, T.; Yokoyama, M.; Okano, T.; Sakurai, Y.; Fukushima, S.; Okamoto, K.; Kwon, G. S. Doxorubicin-loaded poly(ethylene glycol)−poly(b-benzyl-L-aspartate) copolymer micelles: their pharmaceutical characteristics and biological significance. *J. Controlled Release* **2000**, *64*, 143−153.
(31) Upadhyay, K. K.; Le Meins, J. F.; Misra, A.; Voisin, P.; Bouchaud, V.; Ibarboure, E.; Schatz, C.; Lecommandoux, S. Biomimetic doxorubicin loaded polymersomes from hyaluronan-block-poly(gamma-benzyl glutamate) copolymers. *Biomacromolecules* **2009**, *10*, 2802−2808.
(32) Zhou, K.; Wang, Y.; Huang, X.; Luby-Phelps, K.; Sumer, B. D.; Gao, J. Tunable, ultrasensitive pH-responsive nanoparticles targeting specific endocytic organelles in living cells. *Angew. Chem., Int. Ed.* **2011**, *50*, 6109−6114.
(33) Choi, C. H. J.; Alabi, C. A.; Webster, P.; Davis, M. E. Mechanism of active targeting in solid tumors with tranferrin-containing gold nanoparticles. *Proc. Natl. Acad. Sci. U.S.A.* **2010**, *107*, 1235−1240.
(34) Upadhyay, K. K.; Mishra, A. K.; Chuttani, K.; Kaul, A.; Schatz, C.; Le Meins, J. F.; Misra, A.; Lecommandoux, S. The in vivo behavior and antitumor activity of doxorubicin-loaded poly(gamma-benzyl L-glutamate)-block-hyaluronan polymersomes in Ehrlich ascites tumor-bearing BalB/c mice. *Nanomedicine* **2012**, *8*, 71−80.
(35) Yin, H.; Kang, H. C.; Huh, K. M.; Bae, Y. H. Biocompatible, pH-sensitive AB(2) miktoarm polymer-based polymersomes: preparation, characterization, and acidic pH-activated nanostructural transformation. *J. Mater. Chem.* **2012**, *22*, 91968−19178.